Proceedings of the ASME 2014 Pressure Vessels & Piping Division Conference
PVP2014
July 20-24, 2014, Anaheim, CA, USA

Paper number 28223

WELDING DISTORTION CAN BE MITIGATED IF WELDING CURRENT AND TRAVELING SPEED VARY OPTIMIZED ALONG A WELD PATH

Mahyar Asadi
University of Ottawa
Ottawa, ON, Canada

John Goldak
Carleton University
Ottawa, ON, Canada

Arnaud Weck
University of Ottawa
Ottawa, ON, Canada

ABSTRACT

Typically, the distortion from welding is mitigated with the use of fixtures, clamps, tack welds and so on. Also the welding current and traveling speed are normally set constant during welding along a weld-path. The authors have developed and implemented an advanced control method that adaptively changes welding current and traveling speed depending on the state of deformation, in order to mitigate the final distortion without the use of additional hardware such as fixtures, clamps, and/or tack welds. It predicts the distortion before actual happening and adjusts parameters to counteract the deformation during welding. The present work implements this advanced method by applying an optimized, varying welding current and traveling speed on an edge-welded bar of Aluminum 5052-H32. A comparison is made between the final welding distortion with the new method, versus the regular method at constant welding current and traveling speed. A virtual predictive model was established to simulate and control the adaptive change of welding current and traveling speed, the optimized profile of the process parameters were performed by a robot, and the transient distortion was measured by state-of-the-art 3D photogrammetry cameras in real–time.

INTRODUCTION

American Welding Society (AWS) vision of 2020 clearly says that "Welding will move from being an "art" to being a manufacturing science with the help of computers" and talks about the term "virtual factory" where modeling and simulation tools become commonplace in welding operations [1]. Canada's technology roadmap for the Canadian welding and joining industry mentions "Incorporate welding and joining considerations early in product-design stage [using computer models]" [2]. Europeans picture factory of future as "Smart Factories" where advanced automation and control are key technologies to help welding become more competitive, energy-efficient and innovative as part of manufacturing [3]. All of these documents together with the annual reports of IIW (the International Welding Institute), vision statement of the Japanese Welding Engineering Society (JWES), Asian Welding Society (AWS) objectives, and many other documents encourage a conducive environment for expert system of designer-driven control and optimization in welding by help of computer.

Such expert systems lies within the application of artificial intelligence (AI) that falls into two broad categories: a) problem solving and decision making systems, and b) intelligent communication systems [4]. Welding control with use of Laser vision [5] & [6] or thermally scanned welding [7], human-robot interactive welding [8], and sensory feedback control in welding robots [9] & [10] fall into the latter category. Expert systems, however, fall under the former category that is less investigated. A comprehensive literature review on the application of several methods of this category has been summarized by Benyounis and Olabi [11] in the area of welding. They have collected weld optimization applications including Artificial Neural Networks (ANNs), Genetic Algorithm (GA), Response Surface Method (RSM), and Design of Experiment (DOE) to develop a mathematical relationship between the welding process parameters and the objective function(s) of the weld joint ranging from weld-bead geometry to mechanical properties. Success in this category significantly depends on having a reliable predictive model that feasibly and quickly explores large set of design parameters for implementing the modern algorithms of decision-making [12].

Computational weld mechanics (CWM) deals with the models, algorithms, and software to predict the behaviour of welds in the welded structures. CWM started developing early 1970s for practical weld engineering [13] and it is now maturing with a good level of reliability including complex physics of welding, material modelling, and stress-strain dependency on temperature and evolution of microstructure

[14]. Recent activities further has focused on computational strategies and how they are integrated with other approaches to facilitate the use of simulations in industrial scale engineering with sizeable geometry and real-world complexity [15] & [16].

Weld distortion is a frequent problem in various welding applications and many techniques have been developed since 1960s to mitigate the welding distortion [17]. In the past decades, several mitigation methods have been studied using CWM such as pre-deformation [18], thermal tensioning [19] & [20], or by using optimized welding sequences [21], [22] & [23], or surrogate modelling [24] & [25]. Advanced mitigation techniques require hundreds of CWM evaluations for a designer to make a right decision. Increasing power of computation provide a platform for performing more complex algorithm for mitigation of weld distortion such as gradient-free direct search, evolutionary algorithms, or probabilistic metaheuristic that need to be integrated to CWM framework.

From the long list of research work collected by Benyounis and Olabi [11], a few were on the control applications to alleviate the welding distortion during the welding. Arya and Parmar [26], Murugan and Gunaraj [27], Benyounis et al. [28], and Casalino et al. [29] were some of them. Cook et. al. [30] also presented an in-line weld process control application for weld-bead profile control using ANNs modelling. Other than spot welding, there are very few applications that mitigate the distortion or residual stress by optimizing the profile of welding process parameters adaptively during welding.

Recently, authors have developed and implemented an advanced control method that adaptively changes welding current and traveling speed depending on the state of deformation, in order to mitigate the final distortion without the use of additional hardware such as fixtures, clamps, and/or tack welds. It predicts the distortion ahead of actual happening and adjusts parameters to balance it during welding. Therefore, if one has the machinery to apply in-line variation to the welding process parameters such as welding current and speed during welding, then this paper shows that an adaptive control of such parameters could mitigate the distortion.

WELDING EXPERIMENTAL SET-UP

An edge weld on a 1220 x 152 x 12.5 mm bar, shown in Figure 1, was used for the optimization of the welding current profile and speed to mitigate the distortion on the bar. The material was Aluminum 5052-H32 alloy with chemical composition Al 96.7, Mg 2.5, Cr 0.25, Cu max 0.1, Fe max 0.4, Mn max 0.1, Si max 0.25, Zn max 0.1 Wt \%. A robotic gas metal-arc-welding process was employed to weld the specimen's edge and the initial welding parameters were current 127 [amp] positive polarity (DCEP), voltage 15.7 [v], travel speed 7.1 [mm/s], filler metal Al-4043 with 1.6 [mm] wire diameter, wire feed speed 66 [mm/s] and the shielding gas was Argon. Since this is a control problem, the value of the welding current and speed were adjusted along the weld path on the edge of the bar while the welding was progressing. The ratio of the variation in the value of the welding current and speed remained constant in order to keep the power per unit length of weld constant as it sets initially, i.e. 281 [kw/m].

Figure 1 Experimental Set-Up.

The fixture in Figure 1 was designed to constrain the rigid body to zero while positioning the plate's edge in flat weld (1G) with minimal lateral movement. The part was free to deform but one bottom corner was fixed by a side-to-side hole secured with a through screw to the fixture and the other bottom corner was on a rod that allows the plates to slide in longitudinal direction.

The KUKA robot and Fronius welding units, shown in Figure 2, were employed to implement the optimized weld process. Since the deformation was capturing with the photogrammetry cameras, a metallic shield was attached to the fixture and sealed with welding blankets in order to prevent the high intensity light from the welding arc to interfere with cameras' white balance.

Figure 2 KUKA robot and Fronius welding units during welding. A metallic shield prevents the intense light from arc comes to the cameras.

PHOTOGRAMMETRY SET-UP

Photogrammetry or digital image correlation (DIC) tracks the movement of a pattern or applied features on the surface in real-time deformation. A local derivative operator on a series of images taken by high sensitive cameras generates a map of displacement and strain. DIC cameras were used for 2D in-plane map; a set of stereoscopic multi camera can construct a 3D map if needed. The DIC cameras were employed together with robust "DaVis" software from LaVision for capturing experimental deformation and strain map in 2D. Figure 3 shows the cameras when recording the deformation by tracking movement of spackles applied on the bar. The recording was done 5 fps and started before the welding starts and continued after the welding was halted until the plate was cooled down below 50 C (about 20 minutes). Speckle pattern was random but required to cover the surface in proper density of distribution and range of sizes. The optimized pattern is shown in Figure 4.

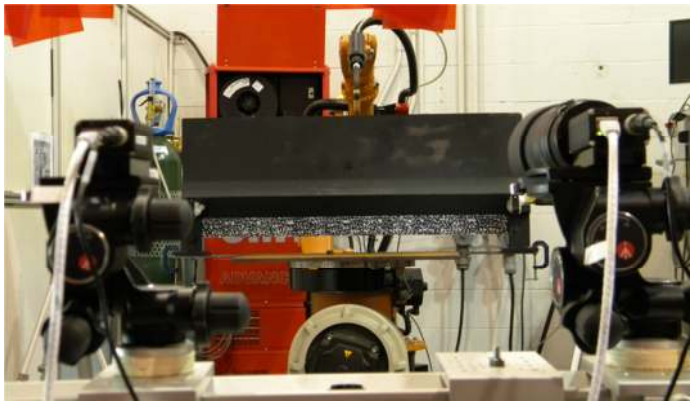

Figure 3 Photogrammetry cameras are recording the motion of the spackle pattern on the Al bar.

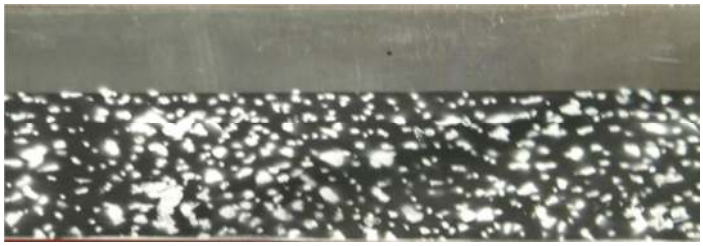

Figure 4 The optimized spackle pattern applied on the plate for photogrammetry. The height of figure represents full width of the bar i.e. 152 [mm].

ADAPTIVE CONTROL SCHEME

The final distortion, if no control or mitigation technique used, forms a camber in the bar so that the maximum occurs in the middle of the bar. The objective is to minimize the maximum deflection in the bar and to reach as a flat bar as possible after the edge welding and cool down.

Welding current and travel speed affect the distortion so that if one can control the welding current and travel speed, an optimized profile of such parameters could alleviate the distortion. An earlier work of ours [4] has been to simulate the use of this idea i.e., adaptive predictive control of welding current and travel speed during welding, in order to mitigate the final distortion. The power per unit length is constrained to be constant and equal to the initial value i.e. 281 [kw/m]. Therefore, the total heat input into the plate is the same from the optimized process versus the traditional process. This is good for distortion comparison since it is an apple-to-apple comparison.

This constraint also couples variations in the welding current and speed. Therefore, the independent control vector can be either the welding current or the travel speed. The welding current was controlled and the traveling speed was adjusted to keep the power per unit length equal to the initial value. As such, the bead size remains visually the same for all segments of weld.

The weld path was divided into 19 sub-paths (64.2 [mm] each) where for each of the weld sub-path the control problem learns from the previous sub-path and tries to find the new value for the welding current and speed that minimize the distortion using predictive Computational Weld Mechanics (CWM). This means that the control algorithm was applied every 64.2 [mm] for 19 times during welding. The only reason for picking every 64.2 [mm] is to save CPU time and the user time to set up the projects and a better result can be achieved by shorter but more sub-paths.

The control algorithm is summarized as follow:

i. Read the welding current, I, and traveling speed, S, from the last time step of the last sub-path.
ii. Perturb the welding current I by 10 % and adjust S to keep the power per unit length constant.
iii. Run the FEM analysis for the next sub-path using three values of the welding current; (I-10% I, I, I+10% I) with adjusted S for each one.
iv. Evaluate the user-defined objective function for the three analyses from the previous step and pick the best configuration.
v. Continue the analysis for the next sub-path using the picked set of I and S from the step v.
vi. Repeat at the end of the sub-path until the end of the welding path.

Readers are encouraged to check reference [4] for details.

The objectives function at step iv was the maximum Y-displacement in the bar. Therefore the best pick was the lowest maximum Y-displacement. A threshold was considered so that the travel speeds are allowed between 4.5 and 10 [mm/s].

Figure 5 The adaptively optimized profile of welding current and traveling speed (solid line) vs. constant ones set at nominal (dotted line).shows the adaptively optimized profile of welding current and travel speed (solid line) as oppose to the typical constant scenario where welding current and travel speed are set at nominal value (dotted line) for the length of weld path. It indicates that an increasing welding current at the beginning and the end of the welding path on an edge welded bar as well as a current level below the nominal in the middle of the bar could result in a bar that is closer to flat compared to

the constant welding current and travel speed. This simulation helps us to understand and remotely optimize welding parameters, but it becomes of practical use when implemented in real world. The main purpose of this paper is to show the successful implementation of such optimized profiles in mitigation of distortion.

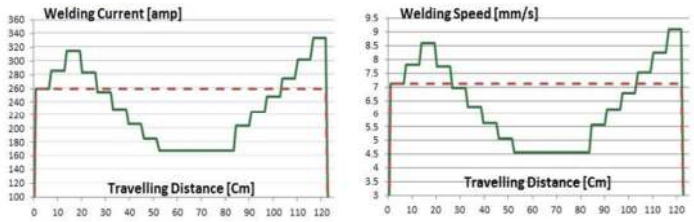

Figure 5 The adaptively optimized profile of welding current and traveling speed (solid line) vs. constant ones set at nominal (dotted line).

The welding current and speed were bounded by maximum and minimum limits. The specimen was allowed to cool to ambient temperature after the welding was completed.

IMPLEMENTATION AND CONSIDERATION

The KUKA robot controls the travel speed and it was programmed to change the speed at every 64.2 [mm] as shown in Figure 5.The robot calls for different scheduled jobs at the end of each step for which power and feeding rate changes. The power i.e. V.I, changes according to the profile shown in Figure 5-left. We found that the welding power used in the simulation was too high because the arc efficiency assumed 60 % and ended in molten edge. The robotic welding machine had much higher efficiency and therefore we implemented a trial test to adjust the power to one third of the values from simulation. The simulation suggests changing power by varying welding current alone for a fixed voltage; however, the actual work changed both welding current and voltage to keep the power to the values from computation as shown in Table 1 (the grey columns). The reason is that the welding machine's constrain (Figure 6 Welding machine's constrain for applying voltage and current.) in changing voltage and current independently was not considered in the control algorithm. The authors believes that the right approach is to re-compute the parameters by re-running the simulation and adaptive control algorithm in order to find a new optimized profile of welding current and travel speed based on efficiency and constraints of the machine used. A further work still is required to be really optimized; however, the profile employed in this experiment deviated not too far from optimum and remains valid to proof of concept that increasing power at both ends along and reducing power in the middle of the bar can mitigate the final distortion.

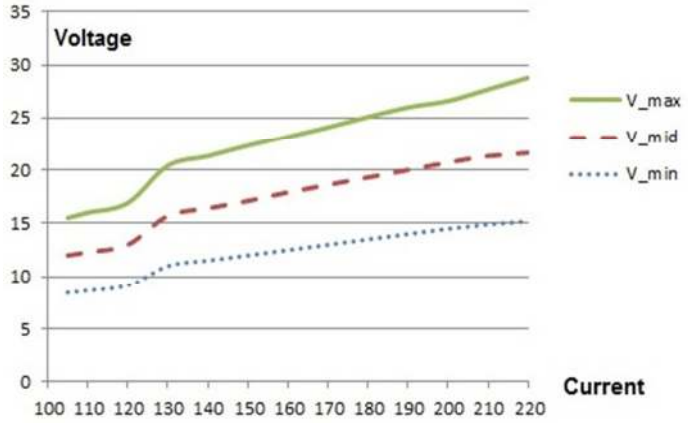

Figure 6 Welding machine's constrain for applying voltage and current.

RESULT AND DISCUSSION

Using higher current (and faster speed) at the beginning and end of welding can potentially mitigates final distortion. Long part of weld bead in the middle of weld path introduces a positive (upward) camber during welding and negative camber as final deflection after cool-down. This suggests (and has proved by many engineers) that lower current results in less distortion. This scenario is no longer true when the weld path is relatively long such that positive cambering in weld location occurs at the same time when negative cambering is in progress at certain distance behind the weld due to cool-down. Therefore the upward deformation at weld counteracts the cool-down deflection, and higher welding current is now helpful, not at the location of weld, but for mitigation of distortion in some distance behind the weld. The welding is continuous process that means although a local increase in welding current helps mitigation of distortion behind the weld, but the deflection is becoming worth at current location of weld unless the weld is approaching the end of the part with no material in front and frees to deform.

Depending on welding problem, there are points that current needs to switch between the increasing and decreasing trend. Finding the right location (or time) of these switches is critical to minimize the final distortion, and a predictive model such as FEM model in necessary.

From simulation, the optimum profile of welding current and travel speed results in the displacement shown in Figure 8. This figure shows that the optimized profile changes the state of deformation from one big bending in the middle of the bar to two smaller ones that are closer to flat and preferred in practical applications. As discussed earlier in this paper, our implementation was not exactly on optimum state and therefore our final measure of deflection is different from this figure. Figure 9 and Figure 10 are the results recorded and analyzed by photogrammetry cameras after welding cool down; figure 7 for deflection from constant welding current and travel speed scenario as oppose to adaptively controlled welding current and travel speed scenario. Both deflections are 25 times magnified in these figures. There are videos associated to each scenario

that show a transient map of deformation. Readers may contact the authors for a copy of these videos. The main difference is that the sinus wave of deflection has not formed in the figure 9 that suggests the amount of increasing power at the beginning of weld path was not high enough to deform the bar significantly in the opposite direction of final deflection. Also the position of switching from increasing trend to decreasing needs to be re-adjusted in order to get a wave-wise deflection. However, the key achievement is that the final deflection is mitigated by almost a factor of two. This shows the effectiveness of this technique as well as suggests that a better control algorithm can be design to push the final deflection toward a wave-wise deflection including one negative deformation in the middle and two small positive at each end.

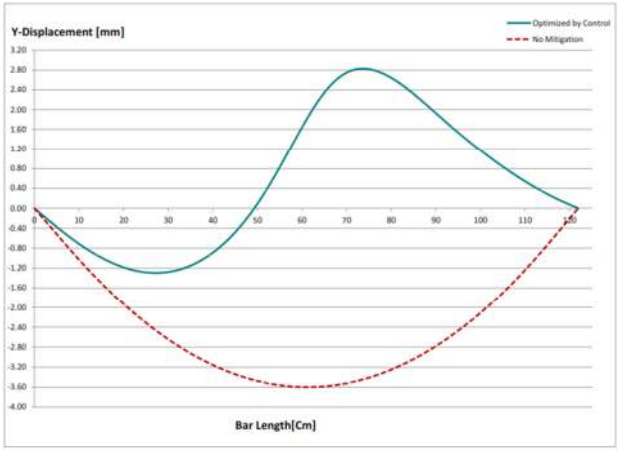

Figure 8 Expected final deflection with no mitigation (dotted line) vs. optimized by control algorithm (solid line) based on preliminary simulation.

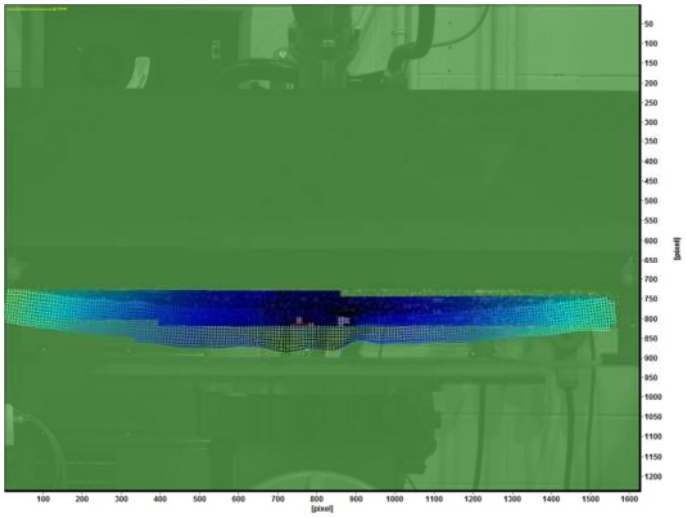

Figure 9 Measured deflection from constant welding current and travel speed scenario (25x magnified).

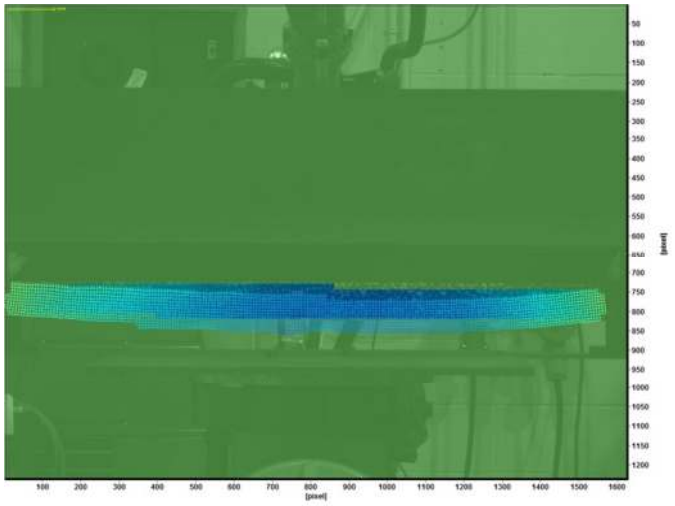

Figure 10 Measured deflection from adaptively controlled welding current and travel speed scenario (25x magnified).

CONCLUSION

An advanced control of welding parameters was shown in this paper for an adaptive control of welding current and speed in order to mitigate the final deflection during welding depending on the state of deformation ahead of actual happening. Digital image correlation (DIC) technique, which was customized for welding, was employed to record the transient map of deformation during welding and cool down. The comparison between the strategy with no application of control and the strategy that uses the control scheme shows the effectiveness of the control scheme. Although the test here is on an edge welded bar and the bar analyzed is a relatively simple structure, the control algorithm is directly applicable to any welded structure. It shows that if one uses higher welding current at the beginning and the end of weld path and stays below the nominal amp in the middle, such a variation leads to less bending distortion at the end. The optimum values of maximum and minimum current together with the location to switch the profile of current requires a robust computational welding mechanics model to help designers find the best arrangement for each weld. However the manual implementation of such analysis takes much expert-user time which is mostly preparation and setup. This manual preparation time can be significantly high in complex and large projects so that the analysis would become unfeasible in practice. An automated framework saves the user's time and drops the total time to the CPU. CPU time per analysis would increase for larger more complex structures but the user's time would change little.

ACKNOWLEDGMENTS

The authors would like to thank Dan Tadic, the director of Canadian Welding Association, for being the main hub of connection between different parties (CWB, KUKA Robotics, Fronius Canada, & Lincoln Electric) in conducting this research. We are particularly grateful for the assistance given

by Ovais Abessi (University of Ottawa) during implementation of tests. We wish to acknowledge the help provided by Stephan Rudd, the senior welding applications specialist from KUKA Robotics, as well as Brian Ronan, welding application technician from Fronius Canada for practical implementation of this research. Also assistance provided by other staff of Fronius Canada (Parkinson Blain and Thompson Rob), and Kuka Robotics (Steve Green and Chris Claring Bold) is greatly appreciated.

REFERENCES

[1] A. W. S. (AWS), "Vision for Welding Industry," American Welding Society (AWS), the United State, 2000.

[2] S. H. Associates, "A Technology Roadmap for the Canadian Welding and Joining Industry," Canadian Welding Bureau (CWB), Canada, 2006.

[3] t. A.-h. I. A. Group, "Factories of the Future PPP, Strategic Multi-Annual Roadmap," European Commission, Europe, 2010.

[4] N. Rajaram, " Expert Systems: the Cutting Edge of Artificial Intelligence," Robotics Engineering, vol. 8, no. 5, pp. 16-20, 1986.

[5] C. S. Wu, D. J. Liu and L. Wu, "An Auto-Programming System of MAG Welding Parameters for Vision-Based Robot," Robotics and Autonomous Systems, vol. 13, pp. 291-296, 1994.

[6] A. Blug, D. Carl, H. Hofler, F. Abt, A. Heider, R. Weber, L. Nicolosi and R. Tetzlaff, "Closed-loop Control of Laser Power using the Full Penetration Hole Image Feature in Aluminum Welding Processes," Physics Procedia, vol. 12, no. A, pp. 720-729, 2011.

[7] Y.-M. Kwak and C. Doumanidis, "Geometry Regulation of Material Deposition in Near-Net Shape Manufacturing by Thermally Scanned Welding," Manufacturing Processes, vol. 4, no. 1, pp. 28-41, 2002.

[8] H. Kazerooni, "Human-Robot Interaction via the Transfer of Power and Information Signals," IEEE Transactions on Systems Man and Cybernetics, vol. 20, no. 2, pp. 450-463, 1990.

[9] D. S. Naidu, S. Ozcelik and K. L. Moore, "Gas Metal Arc Welding: Automatic Control," in Modeling, Sensing and Control of Gas Metal Arc Welding, Idaho, Texas, Utah, Elsevier Ltd, 2003, pp. 147-218.

[10] L. M. Sweet, "Sensor-based control systems for arc welding robots," Robotics and Computer-Integrated Manufacturing, vol. 2, no. 2, pp. 125-133, 1985.

[11] K. Y. Benyounis and A. G. Olabi, "Optimization of Different Welding Processes Using Statistical and Numerical Approaches - A Reference Guide," Advances in Engineering Software, vol. 39, no. 6, pp. 483-496, 2008.

[12] M. Asadi and J. A. Goldak, "Exploring the Parametric Design Space to Manage Weld Distortion Using Design of Experiment," Product Development, Special issue on Simulation-Driven Product Development, vol. 18, no. 1, pp. 31-47, 2013.

[13] L. Lindgren, "Finite Element Modeling and Simulation of Welding. Part 1: Increased Complexity," Journal of Thermal Stresses, vol. 24, no. 1, pp. 141-192, 2001.

[14] L. Lindgren, "Finite Element Modeling and Simulation of Welding. Part 2: Improved Material Modeling," Journal of Thermal Stresses, vol. 24, no. 1, pp. 195-231, 2001.

[15] L. Lindgren, "Finite Element Modeling and Simulation of Welding. Part 3: Efficiency and Integration," Journal of Thermal Stresses, vol. 24, no. 1, pp. 305-334, 2001.

[16] J. A. Goldak and M. Akhlaghi, Computational Welding Mechanics, ISBN-10: 0-387-23287-7: Springer, 2005.

[17] N. Ockerblom, The Calculations of Deformations of Welded Metal Structures, London: Dept. of Scientific and Industrial Research, Translation from Russian, 1958.

[18] M. Asadi and J. A. Goldak, "Mitigation of Distortion in an Edge-Welded-Bar by Clamping Parameters," in the International ASME 2011 Pressure Vessel and Piping Division Conference, Baltimore, Maryland, 2011.

[19] P. Michaleris, J. Dantzig and D. Tortorelli, Welding Journal, pp. 361-366, 1999.

[20] M. Doe and P. Michaleris, "Mitigation of welding induced buckling distortion using transient thermal tensioning," Science and Technology of Welding & Joining, vol. 8, no. 1, pp. 49-54, 2003.

[21] C. L. Tsai, S. C. Park and W. T. Cheng, Welding Journal, vol. 78, no. 5, pp. 157-195, 1999.

[22] M. Mochizuki, M. Hayashi and T. Hattori, "Residual Stress Distribution Depending on Welding Sequence in Multi-Pass Welded Joints With X-Shaped Groove," Pressure Vessel Technology, vol. 122, no. 1, pp. 27-32, 1999.

[23] M. Kadivar, M. H. Jafarpur and H. G. Baradaran, "Optimizing welding sequence with genetic algorithm," Computational Mechanics, vol. 26, no. 1, pp. 514-519, 2000.

[24] I. Voutchkov, A. Keane, A. Bhaskar and T. Olsen, "Weld sequence optimization: the use of surrogate models for solving sequential combinatorial problems," Comput. Methods Appl. Mech. Eng., vol. 194, pp. 30-33, 2005.

[25] M. Asadi and J. A. Goldak, "Combinatorial Optimization of Weld Sequence by Using a Surrogate Model to Mitigate a Weld Distortion," Mechanics and Material in Design, vol. 7, no. 2, pp. 123-139, 2011.

[26] S. K. Arya and R. S. Parmar, "Mathematical Models for Predicting Angular Distortion in CO2-Shielded Flux Cored Arc Welding," in International Conference on Joining of Metals, Helsingor, Denmark, 1986.

[27] V. V. Murugan and V. Gunaraj, "Effects of Process Parameters on Angular Distortion of Gas Metal Arc Welded Structural Steel Plates," in Weld Joint, AWS, 2005, pp. 165-s-171-s.

[28] K. Y. Benyounis, A. G. Olabi and M. S. J. Hashmi, "Residual Stresses Prediction for CO2 Laser Butt-Welding of 304-Stainless Steel," Applied Mechanics and Materials, vol. 3, no. 4, pp. 125-130, 2005.

[29] G. Casalino, S. J. Hu and W. Hou, "eformation Prediction and Quality Evaluation of the Gas Metal Arc Welding Butt Weld," Engineering Manufacturing, vol. 217, no. B, pp. 1615-1622, 2003.

[30] G. Cook, R. J. Barnett, K. Andersen and A. M. Strauss, "Weld Modelling and Control Using Artificial Neural Networks," IEEE Trans Ind Appl, vol. 31, no. 6, pp. 1484-1491, 1995.

TABLE

Table 1 Values for V, I, and S for Computational and Experimental Profile

Step	I_Comp	V_Comp	Speed	Power_Comp	Power_Comp/3	V_Exp	I_Exp	Filler feed (ipm)
1	260.0	23	7.1	5980.0	1993.3	15.7	127	155
2	286.0	23	7.8	6578.0	2192.7	17.3	127	155
3	314.6	23	8.6	7235.8	2411.9	19.0	127	155
4	283.1	23	7.7	6512.2	2170.7	17.1	127	155
5	254.8	23	7.0	5861.1	1953.7	15.4	127	155
6	229.0	23	6.3	5267.0	1755.7	13.8	127	155
7	206.5	23	5.6	4748.6	1582.9	12.5	127	155
8	185.9	23	5.1	4274.6	1424.9	12.6	113	120
9	167.3	23	4.6	3848.1	1282.7	11.4	113	120
10	167.3	23	4.6	3848.1	1282.7	11.4	113	120
11	167.3	23	4.6	3848.1	1282.7	11.4	113	120
12	167.3	23	4.6	3848.1	1282.7	11.4	113	120
13	167.3	23	4.6	3848.1	1282.7	11.4	113	120
14	204.5	23	5.6	4703.3	1567.8	13.9	113	120
15	225.5	23	6.2	5186.5	1728.8	13.6	127	155
16	248.1	23	6.8	5705.2	1901.7	15.0	127	155
17	275.0	23	7.5	6325.0	2108.3	16.6	127	155
18	302.5	23	8.3	6957.5	2319.2	18.3	127	155
19	332.8	23	9.1	7653.3	2551.1	20.1	127	155